DENSE INSTRUMENT ARRAY PROGRAM OF THE PUBLIC WORKS RESEARCH INSTITUTE AND PRELIMINARY ANALYSIS OF THE RECORDS

by

Tadayoshi OKUBO [I], Tadashi ARAKAWA [II] and Kazuhiko KAWASHIMA [III]

SUMMARY

In order to investigate the effects of local geological and topological conditions on earthquake ground motions, usual type of strong motion observation performed at each individual site is not enough, and installation of dense instrument array is indispensable. The Public Works Research Institute, Ministry of Construction, Japan, is now deploying four local laboratory Arrays, consisting of approximately 13 strong motion accelerographs at each site, within four years starting in 1981. This paper presents the dense instrument array program of the Public Works Research Institute, and shows a preliminary analysis of the array data on finite ground strains induced during earthquakes.

INTRODUCTION

Based on the knowledges accumulated through past strong motion observations, it is widely recognized that characteristics of ground motions, especially ground motions in short period, are strongly dependent on source characteristics, path condition between the source and the observation site, and local geological and topological conditions. In view of earthquake ground motions to be used for seismic design of structures, it is of particular interest to investigate the effect of geological and topological conditions on the ground motion. Consequently the Public Works Research Institute formulated a dense instrument array program including deployment of four local laboratory arrays around the Suruga Bay - Izu region which is designated as one of the six high priority sites by the International Workshop on Strong-Motion Earthquake Instrument Arrays(Ref.1). Fig.1 shows the location of the four sites, i.e., Sagara, Yaizu, Numazu and Matsuzaki. This program was initiated in 1981, and deployment of array at Sagara, Yaizu and Numazu has been completed up to the present. The last array at Matsuzaki is scheduled to be deployed in 1984. A total budget of approximately 211 million Yen (approximately 1 million U.S. dollars) is to be invested for the deployment at the four sites.

Furthermore, in order to prepare for these practical observations, two local laboratory arrays consisting of 20 accelerometers were installed in PWRI campus in 1978. The data obtained by this array is presented later in this paper for analysis of finite ground strains induced during earthquakes.

DENSE INSTRUMENT ARRAY PROGRM OF THE PUBLIC WORKS RESEARCH INSTITUTE

Local Laboratory Array at Sagara Site

I. Executive Managing Director, and Chief Engineer, Pacific Consultants International, Shibuya-ku, Tokyo, Japan

II. Head, Ground Vibration Division, Earthquake Disaster Prevention Department, Public Works Research Institute, Ministry of Construction, Tsukuba Science City, Japan

III. Chief Research Engineer, do

Sagara site is located near Omaezaki in Sizuoka Prefecture facing the Suruga-Bay, approximately 170 km south-west of Tokyo as shown in Fig.1. Fig.2 shows instrumentation of the array as well as geological features around the site. Most of the surface of Sagara site is covered by soft alluvium clay deposits. Baserock of this site is Sagara Group, tertiary layers consisted of alternations of sandy and clayey rock, which appears very widely around the site with the shear wave velocity of approximately 700 meter per second. The thickness of the Sagara Group is considered approximately 1 km. Precise investigation of the subsurface ground was conducted based on boring data.

Ten three-components strong-motion accelerographs were installed on the surface along an approximately L-shaped configuration, in which the direction of two legs of L-shaped configuration is selected so that the subsurface ground condition varies along the legs. Four three-components down-hole accelerometers were installed at four points as deep as 36 m so that baserock motions can be obtained. The signals of each down-hole accelerometer are transmitted via cable to the strong-motion accelerographs, which have the same specifications with those installed on the surface.

Thus, used are 14 strong-motion accelerographs which have 4 track digital cartridge recording system. Up to the maximum acceleration of ±1G can be recorded by these accelerographs, and the signals are dizitized with a time interval of 1/200 second by 16 bits AD converter. Pre-event memories of 5 seconds are provided for credit of entire recording of earthquake motions. Time code generators are equipped for each recording system so that exact triggering time can be recorded at the 14 points. It should be noted here that with use of the time code it is possible to get common time basis not only for 14 accelerographs at the Sagara site but also all accle1rographs installed around the Suruga Bay - Izu Region. For the time code generator, auto resetting of the cristal is equipped, which works at each one hour with use of NHK signals so that the error of time code generator be less than 0.01 second. Floating battery chargers are provided with to supply electricity for no shorter than 25 hours in case of suspension of electricity.

Local Laboratory Array at Yaizu Site

Yaizu site is located near Yaizu Port approximately 20 km apart in distance from the Sagara site. The array is consisted of 12 accelerographs set up on the ground and 3 down-hole accelerometers as shown in Fig.3. The left hand site of the Seto river is widely covered by very soft silty materials ap deep as about 110 m, which have the shear wave velocity of about 100m/sec, whereas the right hand side of the Seto river is covered by stiff gravel formations. Thus it is expected that response characteristics of subsurface ground between two sides of the Seto river are much different. The baserock at the site is the Takakusa Group, basalt in Neogene period, which appears at the ground surface at observing point No.1 and is gradually increasing the depth in a direction along observing point Nos.4, 7, 8, 9, 10 and 12. The depth of baserock at the observing point No.9 is about 110 m from the surface, and the deepest down-hole accelerometer is installed at this level. The strong-motion accelerographs, the down-hole accelerometers and time code generators used at this site is the same with those used at Sagara site.

Local Laboratory Array at Public Works Research Institute

Two local laboratory arrays were installed at the Public Works Research Institute, Tsukuba Science City in 1979. Subsurface geological condition around the institute is almost uniform, i.e., dilluvial sandy and silty deposits with approximate thickness of 50 m rest on gravel formations. Shear wave velocities of the upper and lower diluvial deposits are approximately 250m/sec and 400m/sec, respectively.

Fig.4 shows instrumentations at one of the two local laboratory arrays, where 13 three-components accelerometers are installed, i.e., 7 on the surface, 1 at the depth of 2 m, 4 at the depth of 50 m, and 1 at the depth of 46 m, along a cross-shaped configuration with each length of 100 m. The direction of the cross configuration as well as the direction of the sensors is oriented along NS and EW directions. Signals of each sensor are simultaneously transmitted by cable to a central data processing room, where the signals are dizitized with a time interval of 1/100 second by 12 bits AD converter. Thus, the array data with a common time basis can be obtained for analysis.

ANALYSIS OF FINITE GROUND STRAINS WITH USE OF PWRI CAMPUS DATA

Investigations using the array data have been initiated in the Public Works Research Institute on various aspects, such as propagation of seismic waves in horizontal direction, ground strains induced during earthquakes, effects of spatial variation of ground motion on structural response, etc. (Ref.2). As an example of such investigarions, analysis on ground strains induced during earthquakes is presented in the following.

It is evident from past damage experiences caused by destructive earthquakes that damages of extended lifeline systems such as tubular piping systems embedded in ground were most likely caused by relative motions of the ground from point to point in space. Based on these characteristics, the seismic deformation method, which considers ground strains induced during earthquakes as seismic effect instead of inertia forces, was developed and is now in practical use for seismic resistant design of extended structures embedded in ground. Because most of lifeline systems are constructed in a horizontal direction, i.e., x-y plane, with respect to ground, it is of particular interest to estimate normal and shear strains εx, εy, γxy on the horizontal plane due to their predominant influence on the design purpose. Although investigations on actual ground deformations which are developped during earthquakes are essential to assess appropriate seismic effects to be considered in the seismic deformation method, relatively few studies have been made, mostly due to lack of measured data.

Array ovservation has been performed since July 1979 at the PWRI campus, and 21 records as shown in Table 1 have been obtained up to the present. Most of the records were obtained by small earthquake in magnitude which occured around the observing site, but 4 earthquakes have the magnitude of 6 or greater on Richter(JMA) scale.

Fig.5 shows an examples of acceleration time histories recorded by an earthquake of September 25, 1980 (EQ-13, refer to Table 1) which has a magnitude of 6.1 and an epicentral distance to the site of approximately 71 km. Only accelerations at 6 observing ponts, A2C0, A46C0, A50N, A50E, A50S and A50W (refer to Fig.4), are presented in Fig.5. The NS-component at A50N observing point could not be obtained due to malfunction of the data acquisition system. Fig.6 shows the displacement time histories calculated by double integration of acceleration records with the low cut-off frequency of 0.2 second. It is seen from Fig.6 that the acceleration time histories look very similar between the observing ponts of A46C0, A50N, A50E, A50S and A50W, which are almost on the same horizontal plane 50 m below the surface. This can be seen more evidently in the displacement time histories of the ground presented in Fig.6. It is also seen in Fig.6 that the acceleration at A2C0 is appreciably larger in amplitude than that at A46C0 showing amplifications of ground acceleration.

To calculate ground strains, eight tetrahedrons were formulated based on 10 observing points of the array as shown in Fig.7, i.e., 4 tetrahedrons for calculation of lower level ground strains and 4 for calculation of upper level ground strains. In each tetrahedron, the ground displacement u(t), v(t) and w(t) in x(EW), y(NS) and z(UD) directions, respectively, were assumed to be linear. Thus, using a standard finite element analysis procedure for constant strain tetrahedron element, ground strain $\{\varepsilon\}$ defined as

$$\{\varepsilon\} = \{\varepsilon_x, \varepsilon_y, \varepsilon_z, \gamma_{xy}, \gamma_{yz}, \gamma_{zx}\}^T = \{\partial u/\partial x, \partial v/\partial y, \partial w/\partial z, \partial u/\partial y+\partial v/\partial x, \partial v/\partial z+\partial w/\partial y, \partial w/\partial x+\partial v/\partial z\}^T \quad (1)$$

was calculated. It should be noted here that the ground strains considered here by Eq.(1) represent the averaged ground strains between observing points at finite distances. Therefore, the ground strains defined by Eq.(1) are designated hereinafter as finite ground strains.

According to the above-described procedure, the finite ground strains $\{\varepsilon\}$ were calculated using the array data shown in Table 1. Because the records induced by small magnitude earthquakes do not produce meaningful results, only records by earthquakes with magnitude 4 or greater were used for the analysis.

As an example of such calculations, Fig.8 shows time histories of the finite ground strains $\{\varepsilon\}$ at the upper level of zone I calculated for EQ-13. It is seen from Fig.8 that the amplitude of the normal strain ε_x along the horizontal x-axis takes the maximum value of about 50×10^{-6}, which is approximately three times larger than the amplitude of the normal strain ε_y along the horizontal y-axis. The normal strain ε_z along the vertical z-axis is very small. It is also seen from Fig.8 that the time histories of the shear strain γ_{xy} on the horizontal x-y plane are much different in wave shape from the time histories of the shear strains γ_{yz} and γ_{zx} on the vertical y-z and z-x planes. The maximum amplitude of the shear strain γ_{xy} is approximately 60×10^{-6}.

Table 2 tarbulates the maximum amplitude of the finite ground strains for 11 earthquakes. Because the maximum values of the finite ground strains change among the 4 zones, the averages of the maximum finite ground strains over 4 tetrahedrons are presented in Table 2. Ratios of the maximum finite ground strains at the upper level to those at the lower level are also presented in Table 2 to show an amplification with respect to ground depth. It is seen from Table 2 that the upper level finite ground strains are genelally larger than the lower level finite ground strains by a factor of 2 to 5.

With respect to ε_x, ε_y and γ_{xy}, relations between the maximum finite ground strains and the maximum particle velocities of the ground were examined as shown in Fig.9. In this examination, the ground particle velocities at A2C0 and A46C0 were used for correlation of the upper and the lower level finite ground strains, respectively. By least square fitting, one obtaines the relation between the finite ground strains and the particle velocities of the ground as

$$\left.\begin{aligned} \varepsilon &= 20.4 \times v^{0.428} \times 10^{-6} \\ \gamma_{xy} &= 27.5 \times v^{0.810} \times 10^{-6} \end{aligned}\right\} \text{ upper level strains} \quad (1)$$

$$\left.\begin{aligned} \varepsilon &= 12.6 \times v^{0.552} \times 10^{-6} \\ \gamma_{xy} &= 13.2 \times v^{0.518} \times 10^{-6} \end{aligned}\right\} \text{ upper level strains} \quad (2)$$

This relation may be regarded as basic data for assessing the ground strains although it represents only preliminary results baced on a few measured data. It is necessary to accumulate more data through future observation especially the ground motions which develop large ground strains, to improve Eqs.(2) and (3).

CONCLUDING REMARKS

Dense instrument array program of the Public Works Research Institute was briefly introduced. By conducting observations at the array stations described in the preceding section, prompt accumulation of array data caused by large magnitude earthquakes which develop reasonably high accelerations is expected to provide reliable informations about the ground strains.

REFERENCES

1) International Association for Earthquake Engineering: Strong-Motion Earthquake Instrument Arrays, Proc. of the International Workshop on Strong-Motion Earthquake Instrument Arrays, Honolulu, Hawaii, U.S.A., 1978.
2) Okubo, T., Arakawa, T. and Kawashima, K.: Preliminary Analysis of Finite Ground Strains induced during Earthquakes and Effects of Spatial Ground Motion on Structural Response, International Symposium on Lifeline Earthquake Engineering on Pressure Vesseles and Piping Technology, ASME, Oregon, U.S.A., 1983.

Table-1 Array Data Recorded at PWRI

EQ.NO.	DATE	EPICENTER REGION	EPICENTER LONGITUDE	EPICENTER LATITUDE	EPICENTRAL DISTANCE[km]	JMA MAGNITUDE	DEPTH[km]
EQ-1	1979.10.9	OFF IBARAKI	139°50′	36°09′	27	4.1	50
EQ-2	1979.11.25	OFF IBARAKI	140°01′	36°41′	122	5.4	90
EQ-3	1979.12.14	SW IBARAKI PREF.	141°20′	36°45′	156	3.9	40
EQ-4	1979.12.16	E TOCHIGI PREF.	138°57′	35°31′	142	3.0	20
EQ-5	1980. 2.1	–	–	–	–	–	–
EQ-6	1980.4.21	OFF IBARAKI	141°51′	36°02′	198	4.0	60
EQ-7	1980.5.6	–	–	–	–	–	–
EQ-8	1980.5.11	–	–	–	–	–	–
EQ-9	1980.6.18	CENTRAL CHIBA PREF.	140°01′	35°38′	55	4.6	80
EQ-10	1980.6.29	OFF E OF IZU PEN.	139°14′	34°55′	163	6.7	10
EQ-11	1980.9.24	NORTHERN TOKYO MET.	139°42′	36°06′	42	6.0	60
EQ-12	1980.9.25	CENTRAL CHIBA PREF.	140°12′	35°30′	71	6.1	70
EQ-13	SAME WITH EQ-12						
EQ-14	1981.1.28	SW IBARAKI PREF.	139°48′	36°12′	32	Very Small	60
EQ-15	1981.3.12	SW IBARAKI PREF.	140°06′	36°00′	14	About 4	60
EQ-16	1981.9.2	OFF IBARAKI PREF.	141°06′	35°48′	99	6.0	40
EQ-17	1981.9.3	SW IBARAKI PREF.	139°48′	36°06′	25	Very Small	60
EQ-18	1981.9.14	SW IBARAKI PREF.	140°06′	36°06′	3	4.8	70
EQ-19	1981.10.14	SW IBARAKI PREF.	140°00′	36°06′	7	Very Small	50
EQ-20	1981.11.30	SW IBARAKI PREF.	139°54′	36°06′	16	4.2	60
EQ-21	1982.3.7	KASHIMA-NADA	140°40′	36°28′		5.6	60

Note 1) Records of EQ-1~EQ-12 were obtained by temporal recording system with 37 channel analog data recorder.
2) Records of EQ-13~EQ-21 were obtained by digital data acquisitions.
3) EQ-12 is the same earthquake with EQ-13.

Table-2 The Maximum Finite Ground Strains for Upper and Lower Levels.

EQ. NO.	Strains at Lower Level ($\times 10^{-4}$)						Strains at Upper Level ($\times 10^{-4}$)						Strain Ratio (Upper/Lower)					
	ϵ_x	ϵ_y	ϵ_z	γ_{xy}	γ_{yz}	γ_{zx}	ϵ_x	ϵ_y	ϵ_z	γ_{xy}	γ_{yz}	γ_{zx}	ϵ_x	ϵ_y	ϵ_z	γ_{xy}	γ_{yz}	γ_{zx}
EQ-1	10.4	4.9	5.2	11.3	10.4	8.7												
EQ-2	7.55	5.9	6.9	10.7	13.6	14.7												
EQ-6	9.55	8.6	7.2	7.55	15.2	13.4												
EQ-9	5.7	5.4	4.2	6.35	11.4	8.0												
EQ-10	12.4	29.6	9.4	11.1	27.7	26.2												
EQ-11	29.9	–	15.9	–	32.1	37.6												
EQ-13	10.8	14.4	12.4	14.6	–	60.1	39.8	15.4	12.4	56.4	54.2	57.7	3.69	1.07	1.0	3.86	–	0.96
EQ-16	9.0	12.2	14.3	13.0	44.1	31.6	49.4	29.0	14.3	76.7	42.0	37.2	5.49	2.38	1.0	5.90	0.95	1.18
EQ-18	5.0	4.3	4.5	6.15	7.5	13.1	13.7	9.1	4.5	12.0	6.0	13.4	2.74	2.12	1.0	1.95	0.8	1.02
EQ-20	5.8	3.2	3.2	4.9	17.2	7.85	13.6	–	3.2	18.4	17.8	17.7	2.34	–	1.0	3.76	10.3	2.25
EQ-21	10.8	10.9	–	16.7	10.4	78.2	47.5	26.5	–	61.8	79.5	66.4	4.40	2.43	–	3.70	0.76	0.85

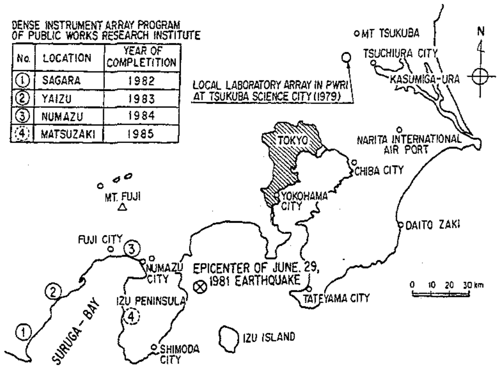

Fig.1 Location of Dense Instrument Array of the Public Works Research Institute

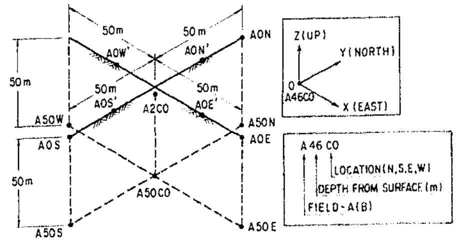

Fig.4 Instrumentation of Local Laboratory Array at PWRI

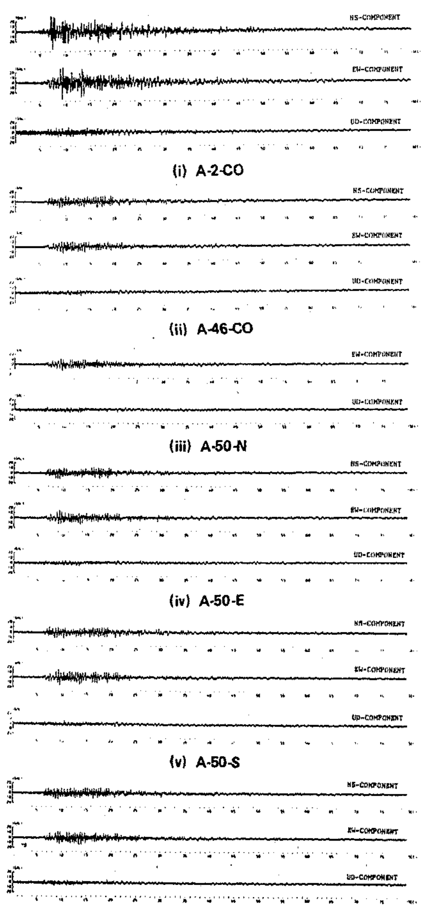

Fig.5 Accelerations by EQ-13

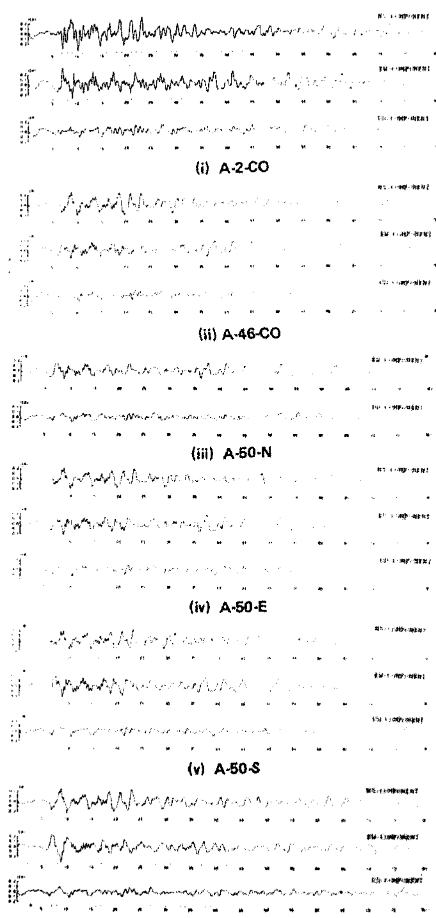

Fig.6 Displacements by EQ-13

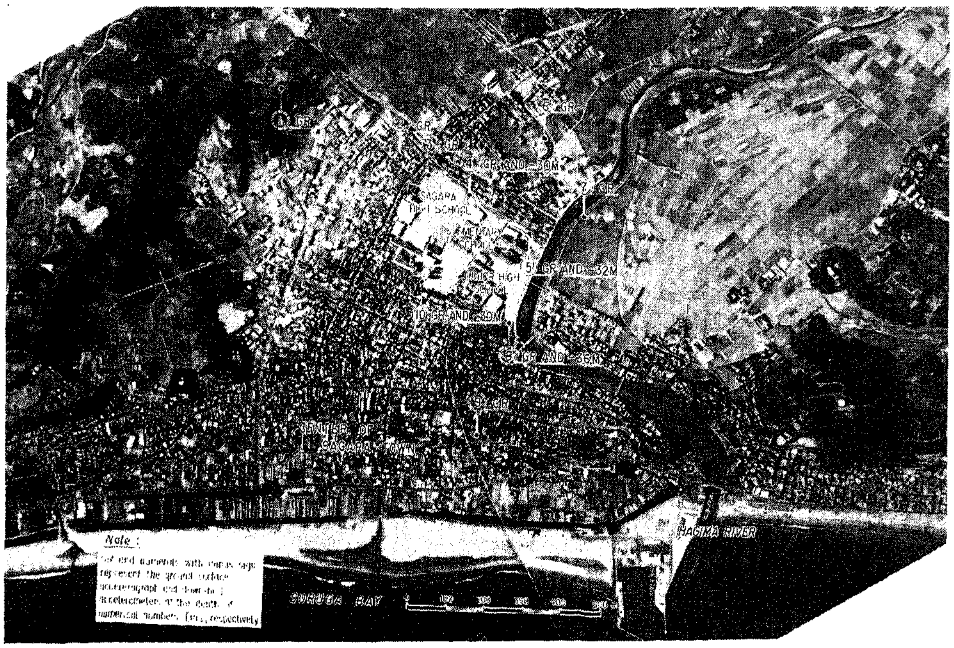

Fig.2 Instrumentation of Array Observation at Sagara Site

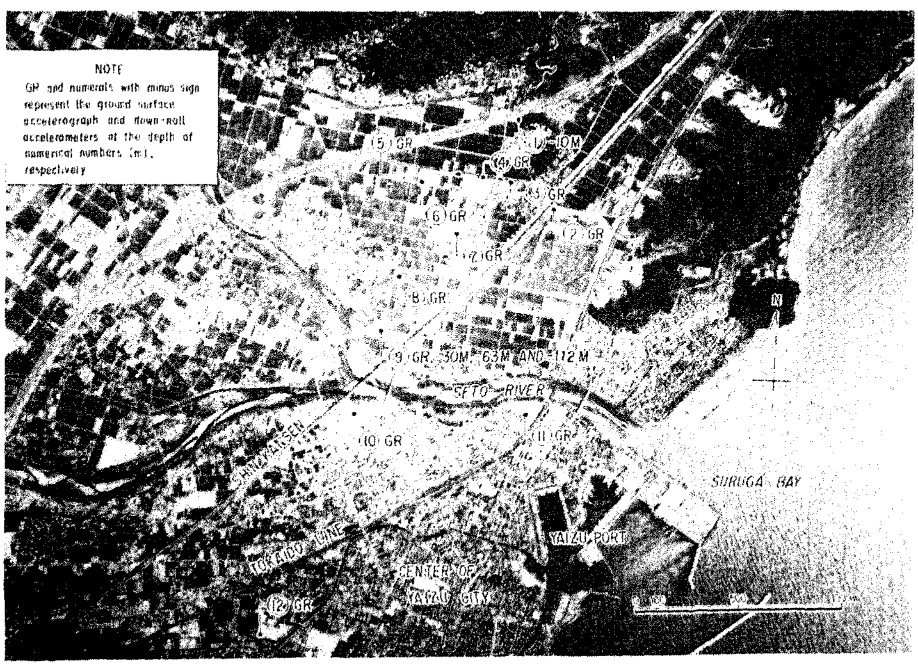

Fig.3 Instrumentation of Array Observation at Yaizu Site

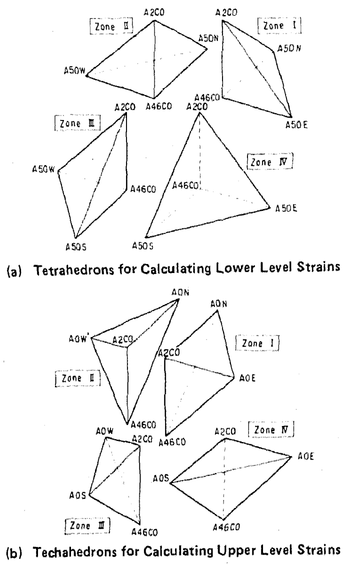

Fig.7
Tetrahedrons Formulated to Calculate Finite Ground Strains

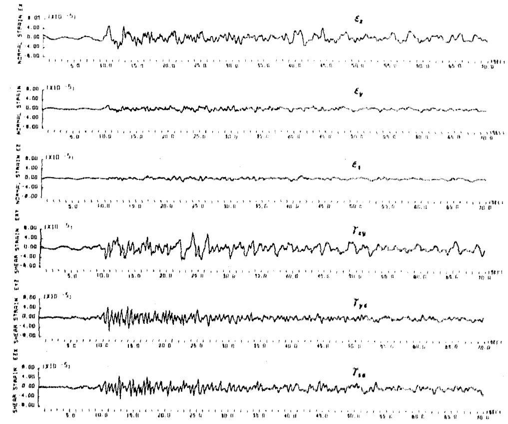

Fig.8
Finite Ground Strains at Upper Level of Zone I Calculated for EQ-13

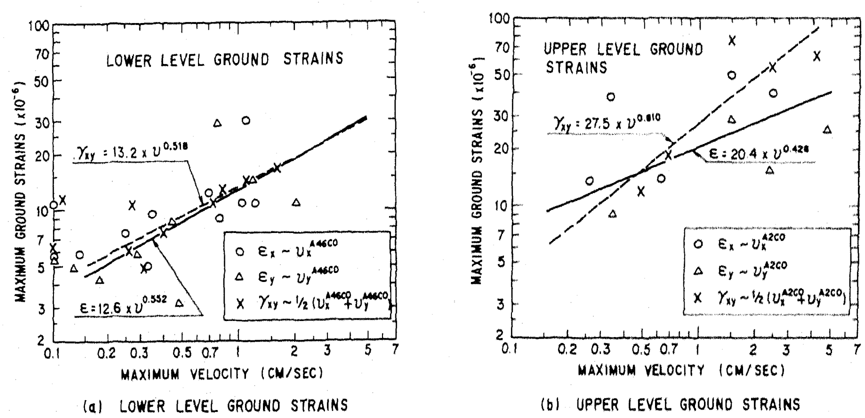

Fig.9
Relation Between the Maximum Finite Ground Strains and the Maximum Particle Velocities